Title

Prospective Pilot Trial to Evaluate a High Resolution Diffusion-Weighted MRI in Prostate Cancer Patients

Authors

Sharif-Afshar, AR
Nguyen, C
Feng, TS
et al.

Publication Date

2016-05-01

DOI

10.1016/j.ebiom.2016.03.041

Peer reviewed

EBioMedicine 7 (2016) 80–84

Contents lists available at ScienceDirect

EBioMedicine

journal homepage: www.ebiomedicine.com

Research Paper

Prospective Pilot Trial to Evaluate a High Resolution Diffusion-Weighted MRI in Prostate Cancer Patients

Ali-Reza Sharif-Afshar [a], Christopher Nguyen [b], Tom S. Feng [a], Lucas Payor [c], Zhaoyang Fan [b], Rola Saouaf [c], Debiao Li [b,d], Hyung L. Kim [a,*]

[a] Division of Urology, Cedars-Sinai Medical Center, Los Angeles, CA, United States
[b] Biomedical Imaging Research Institute, Cedars-Sinai Medical Center, Los Angeles, CA, United States
[c] Department of Radiology, Cedars-Sinai Medical Center, Los Angeles, CA, United States
[d] Department of Bioengineering, University of California Los Angeles, Los Angeles, CA, United States

ARTICLE INFO

Article history:
Received 12 February 2016
Received in revised form 28 March 2016
Accepted 29 March 2016
Available online 8 April 2016

Keywords:
MRI
Prostate cancer
Diffusion weighted imaging

ABSTRACT

Objectives: High-resolution prostate imaging may allow for detection of subtle changes in tumor size, decrease the reliance on biopsies, and help define tumor boundaries during ablation. This pilot clinical trial evaluates a novel high-resolution prostate MRI for detection of small, biopsy-proven prostate tumors.
Methods: Our team developed a software that can be loaded on any modern MRI to generate high resolution diffusion-weighted imaging sequences (HR-DWI), which were compared to standard diffusion-weighted imaging sequence (S-DWI) in a prospective pilot trial in active surveillance patients. HR-DWI captures the entire volume of the prostate rather than sections, reducing streaking artifacts and geometric distortions. Multiple shots, rather than single shots, are used to differentiate signal and noise, enhancing resolution. All images were read by two radiologists. The primary outcome was the percent of biopsy-proven zones seen in 17 patients. The trial was powered to detect discordant proportions of 0.04 and 0.40 at one-sided alpha = 0.05.
Results: The resolution was defined using standard phantoms. HR-DWI produced a 5-fold improvement in spatial resolution when compared to S-DWI. Multiparametric (MP)-MRI incorporating S-DWI was useful for predicting biopsy results (AUC 0.72, Fisher's exact $p < 0.001$); however, using HR-DWI allowed MP-MRI to be more highly predictive of biopsy results (AUC 0.88, Fisher's exact $p < 0.001$). AUC for MP-MRI incorporating HR-DWI was significantly larger than MP-MRI incorporating S-DWI ($p = 0.002$). MP-MRI with HR-DWI had a sensitivity of 95.7% and identified tumor in 22 of 23 zones proven to have cancer on biopsy. In contrast, MP-MRI with S-DWI had a sensitivity of 60.9% and only identified 14 of 23 biopsy-positive zones ($p = 0.004$).
Conclusion: We developed a novel DWI and evaluated its improved resolution in a clinical setting. This technology has many potential applications and should be evaluated in future clinical trials as a patient management tool.

1. Introduction

Transrectal ultrasound-guided (TRUS) biopsy is the gold standard for diagnosing prostate cancer and an integral part of cancer monitoring during active surveillance (AS) (Chen et al., 2016; Mohler et al., 2016). However, the standard prostate biopsy may miss clinically significant disease (Cohen et al., 2008; Kawachi et al., 2010). Furthermore, TRUS biopsy is accompanied by complications such as systemic infection, bleeding, and transient erectile dysfunction (Loeb et al., 2013). There is a clear need for diagnostic strategies to reduce the clinical burden of diagnosing and monitoring prostate cancer. Better imaging may reduce the reliance on biopsies and open but additional therapeutic possibilities.

Multiparametric MRI is commonly employed for detection and localization of prostate cancer (Lawrence et al., 2012; Outwater and Montilla-Soler, 2013). Unfortunately modern MRI suffers from two important limitations. Standard MRI captures periodic slices of tissue and relies on volume averaging, which produces streaking artifacts and geometric distortions. Furthermore, the signal-to-noise ratio on standard MRI limits spatial resolution. To overcome these limitations, we developed a modified three-dimensional, multishot diffusion-weighted imaging sequence (HR-DWI) and applied it in a pilot clinical study. The volumetric imaging improves image quality. Taking multiple shots allows differentiation of signal and noise, further improving resolution.

We choose to test this technology in AS patients who often have low volume disease, which is very often below the limits of detection by

Abbreviations: AS, active surviellance; HR-DWI, high resolution diffusion weighted imaging; S-DWI, standard diffusion weighted imaging; MP-MRI, multiparametric magnetic resonance imaging; ADC, apparent diffusion coefficient; TRUS, transrectal ultrasound.

* Corresponding author at: Cedars Sinai Medical Center, Department of Urology, 8635 West Third Street, Suite 1070 West, Los Angeles, CA 90048, United States.

http://dx.doi.org/10.1016/j.ebiom.2016.03.041

conventional DWI (van As et al., 2009). Although prostate MRI promises to enhance the detection and characterization of prostate cancer, the long-term natural history of small prostate cancers not seen on standard MRI has not been defined. The first step in understanding their biology in an era of molecular diagnostics and next-generation sequencing is to develop technology to image these lesions. Better imaging will allow these lesions to be monitored serially and targeted for biopsy or therapy (Hu et al., 2014). Improved imaging resolution will allow for more accurate measurement of size and boundaries, and detection of small changes in size over time.

Our HR-DWI confers a 5-fold improvement in resolution when compared to standard DWI (S-DWI). The goal of this study is to describe our new imaging system and illustrate its application in a prospective pilot trial of prostate cancer AS patients by comparing the percent of biopsy-proven prostate cancers detected by HR-DWI and S-DWI.

2. Materials and Methods

2.1. Patients

A prospective clinical trial was approved by our institutional review board (IRB). At our center, within the first four years of being diagnosed with prostate cancer, men on active surveillance undergo a repeat prostate biopsy every 1–2 years. Between January 2013 and January 2014, all men scheduled to undergo a prostate biopsy for active surveillance were offered this study (Table 1). After obtaining informed consent, a prostate multi-parametric MRI study with both standard and high-resolution diffusion weighted imaging was performed 2 h before their scheduled prostate biopsy.

2.2. Biopsy and Histological Examination

All patients underwent standard ultrasound-guided transrectal prostate biopsy on the same day using a side-fire biopsy probe (BK Medical Flex Focus 400, Peabody, MA) by a single physician (H.K. with 14 years of experience performing prostate biopsies). Ideally, the reference standard would be provided by pathology from prostatectomy. However, the vast majority of patients with small volume tumors at our institution are managed by active surveillance or watchful waiting, and do not undergo prostatectomy. Therefore, to assess this technology for the detection of small tumors, active surveillance patients were enrolled. A total of 12 biopsy cores were obtained from 6 different regions of the prostate, identified as left/right and base/mid/apex. Our strategy for correlating the 6 prostate zones between MRI and pathology has been described (Feng et al., 2015). Briefly, the prostate was divided into equal thirds and designated anterior, mid and base. The prostate was divided equally into left and right glands. The combination of these two designations allowed radiologists and pathologists to identify 6 discrete prostate zones. All biopsies were reviewed by genitourinary pathologists with expertise in prostate cancer who were blinded to MRI findings.

Table 1

Patient demographics	
Mean age (years)	64
PSA (ng/mL)	
Mean	5.7
Range	0.6–26.9
Stage	
T1c	14
T2a	3
Gleason score at diagnosis	
3 + 3	16
3 + 4	1
Gleason at study biopsy	
Benign	5
3 + 3	9
3 + 4	3
Risk category*	
Very low	5
Low	9
Intermediate	3

* NCCN risk category.

2.3. Imaging and Analysis

A detailed technical description of the new diffusion MRI technique has been published (Nguyen et al., 2015). The previous work dealt with the technical development of the novel high resolution diffusion MRI sequence used in this study. Specifically, it primarily reported on the improvements in image quality (susceptibility-related artifacts, ghosting, geometric distortion, and spatial resolution) and ADC quantification. The present study reports results of the clinical trial, which had over 90% power to detect discordant proportions of 0.04 and 0.40 at one-sided alpha = 0.05 and number of biopsy-positive zones assumed to be 25.

Briefly, the novel diffusion MRI technique was originally developed for in vivo cardiac imaging and translated for prostate imaging (diffusion-prepared balanced steady-state free precession approach that employs 3D multi-shot imaging). Additionally, the 3D multi-shot readout has inherent advantages over 2D single-shot echo-planar imaging used by S-DWI. Advantages include markedly reduced geometric distortion, minimization of susceptibility-related artifacts, and higher achievable spatial resolution. The S-DWI and HR-DWI, at two resolutions, were integrated into a routine multiparametric (MP)-MRI protocol (S-MRI and HR-MRI, respectively), which also included T1 and T2 weighted (T1w and T2w) turbo spin echo sequences and dynamic contrast enhanced (DCE) imaging (Table 2).

Imaging was performed on a 3T MRI system (MAGNETOM Verio, Siemens Healthcare, Erlangen, Germany) equipped with a 12-channel pelvic phased array coil. An endorectal coil was not used. Active surveillance patients were scanned 2-h before their standard 12-core biopsy to avoid edema and hemorrhage-related artifacts induced by the biopsy. Diffusion weighted images (b = 0, 300, 600 s/mm (Mohler et al., 2016): 3 orthogonal directions for each non-zero b-value) were acquired at two prescribed spatial resolutions: One at the typical clinical resolution of 2.1 × 2.1 × 3.5 mm (Cohen et al., 2008) and another at a higher spatial resolution of 0.9 × 0.9 × 3.5 mm (Cohen et al., 2008). Apparent diffusion coefficient (ADC_i) maps were reconstructed offline using Matlab (Mathworks, Natick, MA) assuming a monoexponential fit for each diffusion direction. A final trace apparent diffusion coefficient (ADC) map was calculated ($ADC = [ADC_x + ADC_y + ADC_z]/3$).

Table 2
Specific MR protocol parameters.

	T1w	T2w	DCE	S-DWI		HR-DWI	
				LR	HR	LR	HR
Acquisition readout	2D	2D	2D	2D	2D	2D	3D
TR or TR_g [ms]	692	5850	3.0	4700	10,000	2000	1200
TE or TE_{prep} [ms]	10	125	1.1	80	80	80	80
Echo Spacing [ms]	–	–	3.0	–	–	3.0	3.5
Echo Time [ms]	–	–	1.1	–	–	1.4	1.7
FOV [mm (Mohler et al., 2016)]	150 × 150	150 × 150	250 × 250	220 × 220	180 × 180	220 × 220	180 × 180
Image matrix	250 × 160	320 × 208	192 × 192	104 × 104	208 × 208	104 × 104	208 × 208
Slice thickness [mm]	3.5	3.5	3.5	3.5	3.5	3.5	3.5
Parallel imaging [R]	2	2	2	2	2	2	2
Temporal res [s]	–	–	9.7	–	–	–	–
b-Value [s/mm (Mohler et al., 2016)]	–	–	–	0, 300, 600	0, 300, 600	0, 300, 600	0, 300, 600
Diffusion directions	–	–	–	3	3	3	3
Averages	2	2	1	13	7	1	1
Bandwidth [Hz/pixel]	320	279	698	1502	762	781	801
Scan time	3:06	5:16	9:00	7:32	7:35	7:28	7:32

Imaging resolution was confirmed with a standard spatial resolution American College of Radiology phantom.

Suspicious prostatic lesions were identified and scored according to PI-RADS (Barentsz et al., 2012) by consensus of two genitourinary radiologists (RS: 20 years, LP: 5 years experience in prostate cancer MR characterization) who were blinded to all pathology results and type of DWI protocol (HR vs S). Positive indicators include: hypointensity on T2w, hyperintensity on DWI, hypointensity on ADC, and early wash-in/elevated K_{trans} on DCE. Early wash-in and K_{Trans} was calculated using commercially available Aegis 4D Visualization software (Hologic, San Diego, CA) for prostate. Specific morphological positive indicators include focal or nodule-like regions of the peripheral zone (PZ) and homogenous regions of the transition zone (TZ) absent of clearly delineated margins and capsule. T1w images were used to rule out possible confounding presence of hemorrhage and calcification. The prostate was evaluated once using S-DWI as part of the MP-MRI protocol and then again with the HR-DWI. All lesions with PI-RADS scores greater than three were considered suspicious and subsequently assigned to one of six zones to spatially correspond with the pathology report of the 12-core biopsy.

2.4. Statistical Analysis

The results of the 12-core biopsy were considered the gold-standard reference for the comparison of imaging methods. Study design and data collection was planned prior to study initiation. All patients enrolling in the trial had prior prostate biopsies. Any of the prostate zones were considered positive for cancer if cancer was detected on the study biopsy or any prior biopsy. Measures of diagnostic accuracy, along with 95% confidence intervals were calculated. A $p < 0.05$ was considered significant. Statistical analyses were done with Stata 13.1 (College Station, TX).

3. Results

3.1. Participants

We hypothesized that improved image quality and resolution would allow for better detection of small lesions typically found in patients undergoing active surveillance. Table 1 summarizes the patient demographics for 17 patients in our pilot study. At the time of diagnosis, all patients had Gleason 3 + 3 prostate cancer with the exception of one patient with low-volume Gleason 3 + 4 prostate cancer. Since the study included an MRI exam and prostate biopsy, all patients had at least two 12-core biopsies. Some patients had 3 or more biopsies (6 had 3 biopsies, 2 had 4 biopsies, 1 had 5 biopsies and 1 had 6 biopsies). No patient received treatment for prostate cancer, include 5α reductase inhibitors. A patient was considered to have cancer in a zone of the prostate if cancer was detected in that zone on any prior prostate biopsy.

3.2. Imaging and Analysis

In a previous technical report, we showed that HR-DWI had no susceptibility-related artifacts, significantly less geometric distortion, and better visibility of anatomy (Nguyen et al., 2015). Enhanced spatial resolution for HR-DWI was verified using a standard American College of Radiology phantom (American College of Radiology, 2005). In Fig. 1, the T1 weighted images are provided for visual comparison. HR-DWI was able to resolve the individual holes spaced 1 mm apart but not 0.9 mm apart, indicating a resolution between 0.9 × 0.9 mm (Mohler et al., 2016) and 1.0 × 1.0 mm (Mohler et al., 2016). S-DWI was not able to resolve any of the grids in the figure. The resolution of S-DWI used in our routine clinical setting is 2.1 × 2.1 mm (Mohler et al., 2016). Therefore, HR-DWI improved resolution by a factor of 4.4 to 5.4.

HR-MRI identified tumors that S-MRI did not identify. There were 8 prostate zones from 6 unique patients where biopsy was positive and HR-MRI identified a suspicious lesion but S-MRI was completely negative (Table 3a). Fig. 2 shows representative images of MP-MRI from a patient and it is evident that HR-DWIs have higher resolution when compared to S-DWIs. Similar set of figures is provided for every patient on the clinical trial. Fig. 3 shows the 6 zones of the prostate labeled with number of patients with positive findings from biopsy, S-MRI, and HR-MRI.

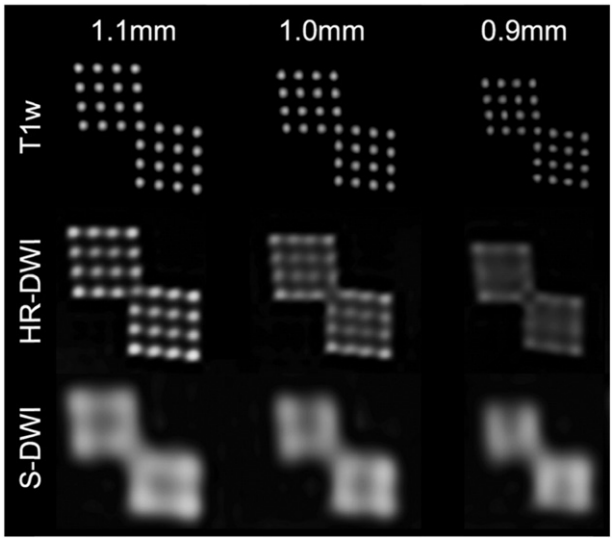

Fig. 1. T1w image, HR-DWI, and S-DWI of a standard spatial resolution American College of Radiology phantom. The T1w image was acquired at higher resolution (0.5 × 0.5 mm, Mohler et al., 2016) for visual comparison. The HR-DWI (0.9 × 0.9 mm, Mohler et al., 2016) and S-DWI (2.1 × 2.1mm, Mohler et al., 2016) were acquired with b value = 600 s/mm (Mohler et al., 2016).

3.3. Statistical Analysis

To illustrate the concordance between S-MRI and HR-MRI, Table 3A shows a 2 × 2 table of MRI findings in prostate zones with biopsy-detected prostate cancer ($p = 0.008$, exact McNemar's significance probability). Table 3b shows a similar table for zones where all biopsies were negative for prostate cancer. There was a high degree of agreement between S-MRI and HR-MRI when the biopsy was negative ($p = 0.500$, exact McNemar's significance probability).

The diagnostic performance of HR-MRI was higher than S-MRI (Table 4). Prostate cancer detection in the 6 zones with biopsies served as the reference standard. Prostate biopsies may not detect all tumors and these test characteristics are provided as exploratory estimates. Both S-MRI and HR-MRI were highly predictive of biopsy results ($p < 0.001$ for both, Fisher's exact test), however the ROC area was significantly higher for HR-MRI when compared to S-MRI ($p = 0.002$, test of equality of ROC areas). Using results from multiple 12-core biopsies minimized sampling error inherent to 12-core prostate biopsy, yet it is still possible that small tumor were missed by the biopsy. However, when a biopsy is positive, there is no doubt that cancer is present. Therefore, it is useful to consider how many of the biopsy-proven zones had abnormal MRI. S-MRI only identified 14 of 23 biopsy-

Table 3a
Status of MRI in zones with biopsy-proved prostate cancer.

Biopsy positive		Standard MRI		
		Negative	Positive	Row total
High resolution MRI	Negative	1	0	1
	Positive	8	14	22
	Column total	9	14	

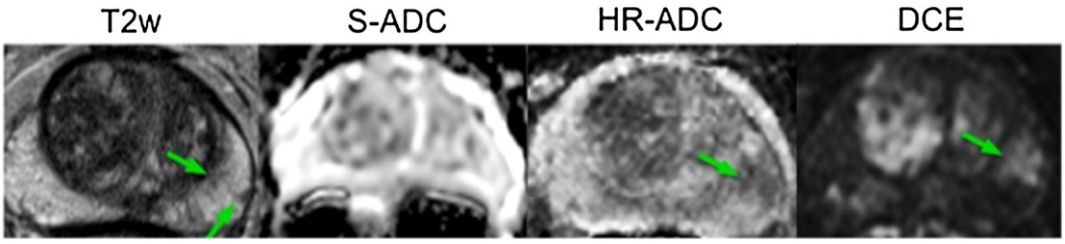

Fig. 2. Representative T2w, S-ADC, HR-ADC, and DCE images for an active surveillance patient enrolled in this study. The arrow highlights the biopsy-proven prostate cancer.

positive zones while HR-MRI identified 22 of 23 such zones ($p = 0.004$, Fisher's exact test).

4. Discussion

Prostate cancer is the most commonly diagnosed cancer in U. S men and the second leading cause of cancer death (Siegel et al., 2014). Active surveillance (AS) has become a standard of care for many patients diagnosed with clinically localized disease. There are various AS strategies employed but most involve repeating PSA measurement and biopsy at regular intervals. Unfortunately, prostate biopsies can be uncomfortable and can be complicated by rectal bleeding, temporary erectile dysfunction, and even sepsis. Therefore, less invasive strategies are needed to monitor prostate cancer on AS. Furthermore, TRUS biopsy has modest sensitivity because up to 85% of prostate cancers are multifocal and 30% of cancers are missed with standard biopsies (Barentsz et al., 2012; Scattoni et al., 2010; Scattoni et al., 2007; Ukimura et al., 2013).

MP-MRI is emerging as a promising tool for detection and noninvasive monitoring of prostate cancer (Stamatakis et al., 2013; Mullins et al., 2013; Panebianco et al., 2014). A recent randomized study by Panebianco et al. explored the incorporation of MP-MPI into a strategy for prostate cancer diagnosis and reported that MP-MRI had an accuracy of 97% for identifying prostate cancer in men with PSA-based criteria suggestive of prostate cancer (Panebianco et al., 2014). The authors also reported that saturation biopsies in men with negative MRI's only identified Gleason 6 cancers or premalignant lesions, implying that lesions not detected on MRI are not clinically significant. Other groups have reported that MP-MRI cannot detect Gleason 3 + 3 prostate cancer in up to 96% of cases if the tumor volume is less than 0.5 cm (Cohen et al., 2008) (Shukla-Dave et al., 2012; Vargas et al., 2012). However, prostate cancer has a long natural history that can only be defined over decades. Furthermore, even higher grade cancers can escape detection on MP-MRI. A recent study by Radtke et al. compared saturation transperineal biopsy with MRI-US fusion targeted biopsies and demonstrated that almost 20% of Gleason 7 or greater tumors are missed if PI-RADS 3–5 lesions are targeted (Radtke et al., 2015). Until we have stronger evidence that small lesions not detected on standard MRI can be safely ignored, even in younger patients, the goal of the research community should be to identify and characterize these lesions.

Medved et al. recently reported on using high-resolution diffusion-weighted imaging of the prostate in 29 patients (Medved et al., 2014). They reported that using 3.1 mm voxels (Cohen et al., 2008), when compared to 6.7 mm voxels (Cohen et al., 2008), produced higher spatial resolution but reduced signal-to-noise ratio. Our imaging technique goes beyond simply reducing voxel size. We use multishot imaging, and signals that persists on multiple images can be designated as true signal and signals that come-and-go can be designated as noise. In our imaging study, the improved resolution resulted from smaller voxels, increased signal-to-noise ratio, and improved image quality associated with volumetric imaging.

Our HR-DWI identified significantly more biopsy-proven lesions than standard diffusion MRI. The ability to visualize these lesions allows clinicians to monitor them serially and follow them for decades if necessary. The MRI technique is made possible by a custom software written by our team and does not require additional hardware. The protocol used in this study added 3.5 additional minutes of scan time to produce a 5-fold increase in spatial resolution for a total scan time of 7.5 min.

In our study, suspected lesions were categorized using PI-RADS, version 1 (Barentsz et al., 2012). PI-RADS, version 2 has recently been released (American College of Radiology, 2015). In this version, nearly all cancers are identified and scored on DWI and findings on T2 images are not factored into the final assessment at all. DCE images are only used to differentiate between some PI-RADS 3 and 4 lesions. Our MRI sequence specifically improves the DWI and the ADC maps, making it potentially more useful for the latest version of PI-RADS. However, until the new PI-RADS version has been clinically validated we chose to report this study using the earlier version.

An important limitation of our study is that radical prostatectomies were not available for the majority of patients and the reference standard was provided by 12-core biopsies. However, biopsy results can serve as a "gold standard" when the endpoint is the MRI-detection of biopsy-proven lesions. We believe this endpoint is appropriate in a pilot study designed to assess whether this technology should be

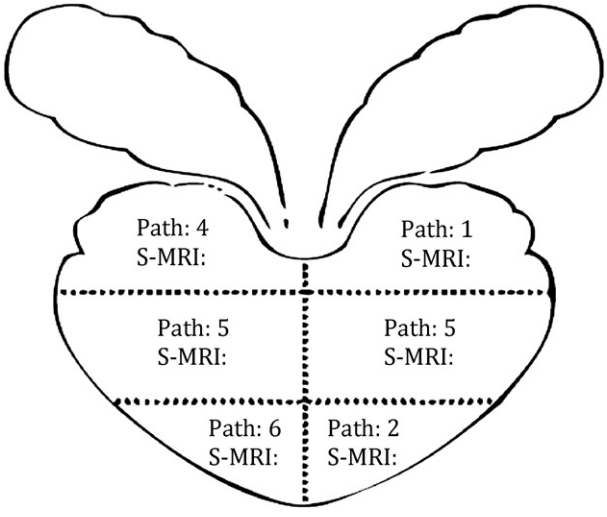

Fig. 3. Diagram showing the 6 prostate zones. The number of cases considered positive for prostate cancer by prostate biopsy, standard (S) MRI, and high resolution (HR) MRI are shown.

Table 3b
Status of MRI in zones where biopsies were negative for prostate cancer.

Biopsy negative		Standard MRI		
		Negative	Positive	Row total
High resolution MRI	Negative	64	0	64
	Positive	2	13	15
	Column total	66	13	

Table 4

Diagnostic characteristics of multiparametric MRI for predicting biopsy results (n = 90 prostate zones)

MP-MRI containing:	Fisher's exact p[a]	Sensitivity[c]	Specificity[c]	ROC area[b]	PPV[c]	NPV[c]
S-DWI	$p < 0.001$	60.9% (38.5–80.3)	83.5% (73.5–90.9)	0.72	51.9% (31.9–71.3)	88.0% (78.4–94.4)
HR-DWI	$p < 0.001$	95.7% (78.1–99.9)	81.0% (70.6–89.0)	0.88	59.5% (42.1–75.2)	98.5% (91.7–100.0)

Abbreviations: MP = multiparametric, S-DWI = standard diffusion weighted image, HR-DWI = high resolution diffusion weighted image, ROC = receiver operating characteristic, PPV = positive predictive value, NPV = negative predictive value.

[a] p-Value for contingency table of biopsy and MRI results.

[b] p-Value comparing ROC areas = 0.002.

[c] 95% confidence interval.

further developed for clinical use. An important goal of the study was to assess HR-MRI for detecting small-volume disease. Therefore, we studied active surveillance patients and not the modern prostatectomy candidates who tend to have bulky disease. Also, MRI-targeted biopsies were not used since MRI-targeting implies that the lesion was visible on standard MRI, and we were interested in developing a technology that could find lesions and tumor boundaries not previously seen on standard MRI. Another limitation is that it may not be possible to blind radiologists to the type of DWI and that the same two radiologists read both S-MRI and HR-MRI, leaving open the possibility that results of one MRI influenced reporting of the other MRI; however, we were willing to accept this possibility since this effect is only likely to falsely enhance the reported accuracy of S-MRI and not HR-MRI.

5. Conclusion

HR-DWI provided higher spatial resolution and improved image quality that resulted in better detection of prostate cancer in AS patients. The ability to image small lesions is the first step in serially monitoring the lesions and defining their long-term natural history, as well as targeting them for biopsy, therapy and molecular characterization.

Authors' Contributions

Ali-Reza Sharif-Afshar: literature search, figures, study design, data collection, data analysis and interpretation, writing.

Christopher Nguyen: study design, data collection, data analysis and interpretation, writing.

Tom S. Feng: data collection, analysis, writing.

Zhaoyang Fan: data collection, analysis and interpretation.

Lucas Payor: data collection, analysis and interpretation.

Rola Saouaf: data collection, analysis and interpretation.

Debiao Li: study design.

Hyung L. Kim: study design, data analysis, interpretation, figures and writing.

Disclosure

All authors have no relevant financial or nonfinancial relationships to disclose.

Acknowledgements

The project described was supported by the Lauhlere Family Fund and the National Center for Advancing Translational Sciences, Grant UL1TR000124 and NIH Grant 1F31EB018152-01A1. The content is solely the responsibility of the authors and does not necessarily represent the official views of the NIH.

References

American College of Radiology, 2005. Phantom Test Guidance.
American College of Radiology, 2015. MR Prostate Imaging Reporting and Data System Version 2.0.
Barentsz, J.O., Richenberg, J., Clements, R., et al., 2012. ESUR prostate MR guidelines 2012. Eur. Radiol. 22, 746–757.
Chen, R.C., Rumble, R.B., Loblaw, D.A., et al., 2016. Active surveillance for the management of localized prostate cancer (Cancer Care Ontario Guideline): American Society of Clinical Oncology Clinical Practice Guideline Endorsement. J. Clin. Oncol.
Cohen, M.S., Hanley, R.S., Kurteva, T., et al., 2008. Comparing the Gleason prostate biopsy and Gleason prostatectomy grading system: the Lahey Clinic Medical Center experience and an international meta-analysis. Eur. Urol. 54, 371–381.
Feng, T.S., Sharif-Afshar, A.R., Smith, S.C., et al., 2015. Multiparametric magnetic resonance imaging localizes established extracapsular extension of prostate cancer. Urol. Oncol. 33 (109), e15–e22.
Hu, J.C., Chang, E., Natarajan, S., et al., 2014. Targeted prostate biopsy in select men for active surveillance: do the Epstein criteria still apply? J. Urol. 192, 385–390.
Kawachi, M.H., Bahnson, R.R., Barry, M., et al., 2010. NCCN clinical practice guidelines in oncology: prostate cancer early detection. J. Natl. Compr. Canc. Netw. 8, 240–262.
Lawrence, E.M., Gnanapragasam, V.J., Priest, A.N., et al., 2012. The emerging role of diffusion-weighted MRI in prostate cancer management. Nat. Rev. Urol. 9, 94–101.
Loeb, S., Vellekoop, A., Ahmed, H.U., et al., 2013. Systematic review of complications of prostate biopsy. Eur. Urol. 64, 876–892.
Medved, M., Soylu-Boy, F.N., Karademir, I., et al., 2014. High-resolution diffusion-weighted imaging of the prostate. AJ. Am. J. Roentgenol. 203, 85–90.
Mohler, J.L., Armstrong, A.J., Bahnson, R.R., et al., 2016. Prostate cancer, version 1.2016. J. Natl. Compr. Canc. Netw. 14, 19–30.
Mullins, J.K., Bonekamp, D., Landis, P., et al., 2013. Multiparametric magnetic resonance imaging findings in men with low-risk prostate cancer followed using active surveillance. BJ. Int. 111, 1037–1045.
Nguyen, C., Sharif-Afshar, A.R., Fan, Z., et al., 2015. 3D high-resolution diffusion-weighted MRI at 3T: preliminary application in prostate cancer patients undergoing active surveillance protocol for low-risk prostate cancer. Magn Reson Med.
Outwater, E.K., Montilla-Soler, J.L., 2013. Imaging of prostate carcinoma. Cancer Control 20, 161–176.
Panebianco, V., Barchetti, F., Sciarra, A., et al., 2014. Multiparametric magnetic resonance imaging vs. standard care in men being evaluated for prostate cancer: a randomized study. Urol. Oncol.
Radtke, J.P., Kuru, T.H., Boxler, S., et al., 2015. Comparative analysis of transperineal template saturation prostate biopsy versus magnetic resonance imaging targeted biopsy with magnetic resonance imaging-ultrasound fusion guidance. J. Urol. 193, 87–94.
Scattoni, V., Zlotta, A., Montironi, R., et al., 2007. Extended and saturation prostatic biopsy in the diagnosis and characterization of prostate cancer: a critical analysis of the literature. Eur. Urol. 52, 1309–1322.
Scattoni, V., Raber, M., Abdollah, F., et al., 2010. Biopsy schemes with the fewest cores for detecting 95% of the prostate cancers detected by a 24-core biopsy. Eur. Urol. 57, 1–8.
Shukla-Dave, A., Hricak, H., Akin, O., et al., 2012. Preoperative nomograms incorporating magnetic resonance imaging and spectroscopy for prediction of insignificant prostate cancer. BJ. Int. 109, 1315–1322.
Siegel, R., Ma, J., Zou, Z., et al., 2014. Cancer statistics, 2014. CA Cancer J. Clin. 64, 9–29.
Stamatakis, L., Siddiqui, M.M., Nix, J.W., et al., 2013. Accuracy of multiparametric magnetic resonance imaging in confirming eligibility for active surveillance for men with prostate cancer. Cancer 119, 3359–3366.
Ukimura, O., Coleman, J.A., de la Taille, A., et al., 2013. Contemporary role of systematic prostate biopsies: indications, techniques, and implications for patient care. Eur. Urol. 63, 214–230.
van As, N.J., de Souza, N.M., Riches, S.F., et al., 2009. A study of diffusion-weighted magnetic resonance imaging in men with untreated localized prostate cancer on active surveillance. Eur. Urol. 56, 981–987.
Vargas, H.A., Akin, O., Shukla-Dave, A., et al., 2012. Performance characteristics of MR imaging in the evaluation of clinically low-risk prostate cancer: a prospective study. Radiology 265, 478–487.